EPJ E
Soft Matter
www.epj.org

Eur. Phys. J. E **26**, 137–142 (2008) DOI: 10.1140/epje/i2007-10259-3

Bacterium organizes hierarchical amorphous structure in microbial cellulose

S. Koizumi, Z. Yue, Y. Tomita, T. Kondo, H. Iwase, D. Yamaguchi and T. Hashimoto

EDP SCIENCES
Società Italiana Di Fisica
Springer

Eur. Phys. J. E **26**, 137–142 (2008)
DOI 10.1140/epje/i2007-10259-3

THE EUROPEAN PHYSICAL JOURNAL E

Bacterium organizes hierarchical amorphous structure in microbial cellulose

S. Koizumi[1,a], Z. Yue[1], Y. Tomita[2], T. Kondo[2], H. Iwase[1], D. Yamaguchi[1], and T. Hashimoto[1]

[1] Advanced Science Research Center, Japan Atomic Energy Agency, Tokai, Ibaraki 319-1195, Japan
[2] Bio-Architecture Center and Graduate School of Bioresource and Bioenviromental Sciences, Kyushu University, 6-10-1 Hakozai, Higashi-ku, Fukuoka, Fukuoka 812-8581 Japan

Received 31 October 2007 and Received in final form 12 December 2007
Published online: 3 March 2008 –

Abstract. A *pellicle*, a gel film of microbial cellulose, is a supermolecular system containing 99% of water by weight, which is closely related to an amorphous structure in it. Using ultra-small–angle neutron scattering, in order to cover over a wide range of length scales from nm to 10 μm, we examined the hierarchical amorphous structure in the microbial cellulose, which is synthesized by a bacterium (*Acetobacter xylinum*). The microbial cellulose swollen by water shows small-angle scattering that obeys a power law q-behavior according to $q^{-\alpha}$ as a function of the magnitude of the scattering vector q. The power law, determined by scattering, is attributed to a mass fractal due to the distribution of the center of mass for the crystallite (microfibril) in amorphous cellulose swollen by water. As q increases, α takes the values of 2.5, 1, and 2.35, corresponding, respectively, to a gel network composed of bundles, a bundle composed of cellulose ribbons, and concentration fluctuations in a bundle. From the mass fractal q-behavior and its length scale limits, we evaluated a volume fraction of crystallite in microbial cellulose. It was found that 90% of the cellulose bundle is occupied by amorphous cellulose containing water.

PACS. 66.30.hk Polymers – 64.75.Yz Self-assembly

1 Introduction

Cellulose is the most abundant biopolymer on Earth, synthesized by a wide variety of living organisms as well as by higher plants [1]. It is a linear homopolysaccharide, composed of β-1,4-linked glucans with a high level of symmetry in an amphiphilic molecular structure. Interchain hydrogen bonding makes cellulose crystalline and therefore insoluble in water, and intrachain hydrogen bonding makes it stiff. The crystallite (or microfibril) in the cellulose texture excludes water molecules and is crucial for physicochemical stability.

The water-soluble nature of cellulose, on the other hand, is necessary for organisms to live in aqueous environments. The affinity to water is closely related to amorphous domains, hierarchically organized in the cellulose texture, where *amorphous* refers to a space occupied by the cellulose swollen by water or by pure water. Microscopic and crystallographic examinations of cellulose microfibrils from different organisms have revealed that the size of microfibrils varies greatly among different organisms [1].

[a] e-mail: koizumi.satoshi@jaea.go.jp

In this paper, we investigate the hierarchical amorphous structure in *pellicles* (microbial cellulose gel) produced by the bacterial species *Acetobacter xylinum*. The pellicle is a supramolecular system, surprisingly containing up to 99% water by weight. The formation of hierarchical structures in the pellicle involves nearly simultaneous and subsequent processes of polymerization, crystallization, and assembly. These processes are controlled by combined factors of i) the highly symmetric and stiff molecular structure of β-1,4-linked glucans, ii) biogenesis by prokaryotic *and* aerobic genera, and iii) physicochemical factors controlling cultivation processes (temperature, agitation etc.). This is a new topic of soft-matter science as a non-equilibrium open system.

A. xylinum, which is a gram-negative and aerobic bacterium, synthesizes an extracellular fibril of cellulose in association with a row of a complex of proteins called the *terminal complex* (TC) in the outer membrane of the cell [1]. Figure 1 shows a schematic diagram of *A. xylinum* and the hierarchical structures found in the cellulose pellicle. This prokaryotic bacterium uses glucose in medium culture and changes glucose into UDP-glucose (UDPG) in the cytoplasm. A row of about 60 TCs located on the outer membrane of the cell are responsible for the recognition and synthesis of UDPG, then the

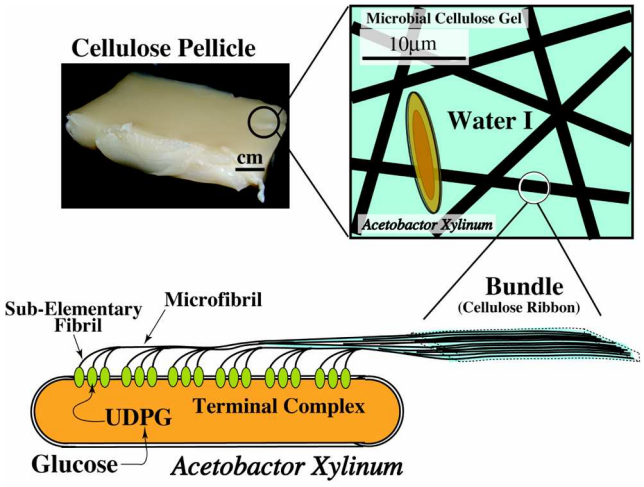

Fig. 1. Schematic diagram of *Acetobactor xylinum* and hierarchical structures found in microbial cellulose.

crystallization and extrusion of cellulose fibers. Extruded from each TC is a *sub-elementary fibril*, composed of 6 chains of β-1,4-glucan [1]. In the sub-elementary fibril, we find a metastable crystalline polymorph of Cellulose I, in which the glucan chains are parallel to each other. The sub-elementary fibrils extruded from neighbors along the row of TCs assemble into a *microfibril* and further into a *cellulose ribbon*, and finally accumulate into a pellicle that floats on top of the culture medium and entraps *A. xylinum*.

One of the most interesting phenomena reported so far is that the synthesis of linear polysaccharide chains can be involved in generating movement of entire cells. Cellulose synthesis in the bacterial cell gives rise to a rotational movement of the cells along their longitudinal axes as they spin the cellulose ribbon. This movement is thought to be due to the force of cellulose microfibril crystallization (crystallization is a source of energy for mechanical force generation). Growing cellulose microfibrils, provided by plant cells, also give rise to forces. However, unlike the microbial cells, plant cells are part of multicellular organisms and therefore do not move about their axis.

For the purpose of this paper, we employed an ultra-small–angle and a small-angle neutron scattering technique (USANS and SANS). The combination of USANS and SANS is advantageous for *in situ* observation over for a wide range of length scales from nm to 10 μm. This method enabled us to examine the cellulose without drying or staining. If we simply replace water with its deuterated form (D_2O), neutron scattering visualizes the spatial distribution of the center of mass for a crystallite in amorphous domains of a microbial cellulose gel. For the swollen cellulose, we found that small-angle scattering obeys a power law q-behavior according to $q^{-\alpha}$ as a function of the magnitude of the scattering vector q. The power law, determined by scattering, is attributed to the mass fractal due to the distribution of the center of mass for the crystallite (microfibril) in amorphous cellulose swollen by water. Finally, from the mass fractal q-behavior and its length scale limits, we evaluated a volume fraction of crystallite in microbial cellulose.

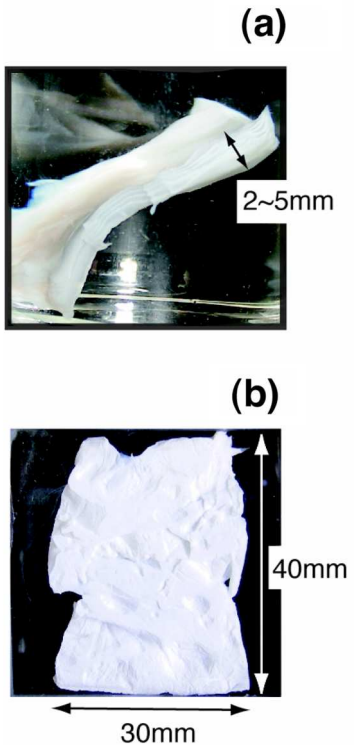

Fig. 2. The film specimen of (a) cellulose swollen by D_2O and (b) dried cellulose.

2 Experimental

2.1 Preparation of microbial cellulose

Acetobacter xylinum, coded as ATCC strain 53582 (NQ-5), was cultivated in a petri dish containing 200 cc of the Hestrin-Schramm (HS) culture medium (pH = 6.0). After incubation for 2 weeks at 30 °C, we obtained a pellicle of 1 cm thickness, floating on the top of the culture medium. To obtain pure cellulose not containing bacteria, we cut the air side of the pellicle into a film specimen of 2–5 mm thickness. We examined two film specimens of microbial cellulose: a) swollen by water and b) dried completely (see Fig. 2). In order to obtain a large scattering contrast, the film specimen of cellulose, cultivated in the HS culture medium in H_2O, was first immersed in a large amount of D_2O over several nights and H_2O was replaced with D_2O. After SANS and USANS measurements, water in the film specimen was completely evaporated in a vacuum oven. The height and width of the film specimen was not greatly changed by drying (height and width = $40 \times 30\,\mathrm{mm}^2$). The weight fraction of dried cellulose was determined from the weight of cellulose film shown in Figure 2(b) (= 0.0033 g) as 5.5 wt%.

We then homogenized the cellulose pellicle in a homogenizer (Histocolon). After drying, the specimen was

stained. The cellulose pellicle was examined by transmission electron micrography (TEM).

2.2 Neutron scattering

We employed two USANS spectrometers at the research reactor JRR-3, at the Japan Atomic Energy Agency, Tokai, Japan. A focusing USANS spectrometer (SANS-J-II) was newly constructed using a focusing compound lens (MgF_2) to cover a q-region of USANS ($10^{-4} < q < 0.003\,\text{Å}^{-1}$) [2], where q is defined as $q = 4\pi/\lambda \sin(\theta)$ with scattering angle 2θ and wavelength λ. With the SANS-J-II, conventional pinhole collimations may be employed without using focusing lenses, in order to cover $0.003 < q < 0.1\,\text{Å}^{-1}$ by changing the sample-to-camera distance. In order to reach a USANS q-region of the order of $10^{-5}\,\text{Å}^{-1}$, we utilized a double-crystal (Bonse-Hart) USANS spectrometer (PNO) at JRR3, Tokai. Using grooved perfect silicon crystals and thermal neutrons of $\lambda = 2\,\text{Å}$, we can cover from 3×10^{-5} to $10^{-4}\,\text{Å}^{-1}$. Due to the line shape of the incident neutron beam, it is necessary to compensate for a smearing effect. Calibration to obtain absolute differential scattering cross-sections was done first for conventional SANS using a secondary standard, irradiated Al and a film of polymer blend, conforming to Porod's law of scattering ($\sim q^{-4}$) with macrophase separation with a sharp interface boundary. Then USANS obtained by SANS-J-II or by PNO was shifted to smoothly connect the calibrated scattering curve for conventional SANS.

3 Experimental results and discussion

3.1 Transmission electron microscopy

Figure 3 shows a TEM image obtained for the dried cellulose. We can recognize the cellulose ribbons, whose width ranges from 50 to 100 nm. The individual ribbons are preferentially orientated from top to bottom in the figure. A thin bridge of cellulose can be seen between two ribbons, as indicated by the arrow. Although the effect of cutting the sample might not be negligible, these structures, composed of cellulose ribbons, form a bundle structure, which is discussed later with respect to USANS.

3.2 Neutron scattering

Figure 4 shows USANS and SANS q-profiles, obtained for the swollen and dried cellulose. The USANS q-region from 3×10^{-5} to $3 \times 10^{-4}\,\text{Å}^{-1}$ was observed by PNO, whereas q-regions from USANS to SANS, corresponding to 3×10^{-4} to $0.1\,\text{Å}^{-1}$, were observed by SANS-J-II. We stress here that focusing USANS, achieved with MgF_2 lenses on SANS-J-II, plays a crucial role to cover from 3×10^{-4} to $3\times 10^{-3}\,\text{Å}^{-1}$, which has been a gap between the Bonse-Hart double-crystal USANS and pinhole SANS spectrometers. The scattering intensities of swollen and dried cellulose

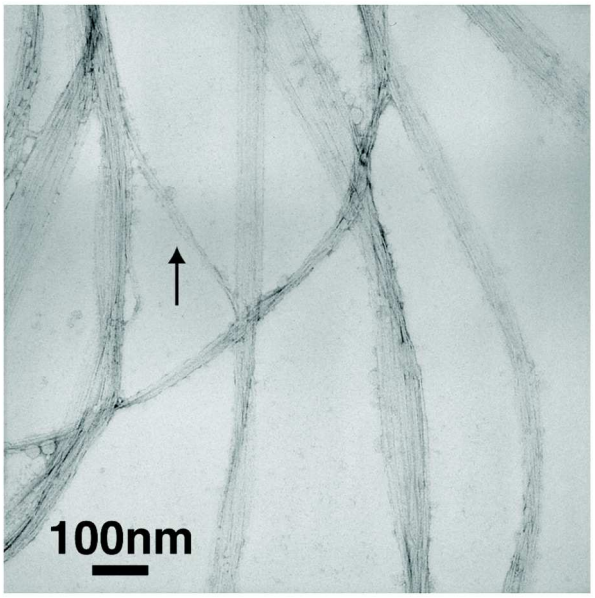

Fig. 3. Transmission Electron Micrography (TEM) image obtained for cellulose ribbons.

were shifted to each other, in order to clearly show those q-behaviors.

For the swollen cellulose (open squares in Fig. 4), the scattering curve exhibits a characteristic power law q-behavior ($\sim q^{-\alpha}$). From higher q values, we found $\alpha = 2.35$ for $0.001 < q < 0.07\,\text{Å}^{-1}$, $\alpha = 1$ for $0.0003 < q < 0.001\,\text{Å}^{-1}$, and $\alpha = 2.5$ for $0.00003 < q < 0.0003\,\text{Å}^{-1}$, respectively. The upper and lower limits for the power laws are denoted as q_1, q_2, q_3 and q_4, respectively, in Figure 4. At q_1 or q_3, there is a hump or drop, respectively, deviating from the power laws.

We attribute $\alpha = 1$ found in the middle q-region ($q_3 < q < q_2$) to a bundle composed of the cellulose ribbons swollen by water. The shape of the bundle is one-dimensional and rod-like. q_2, the upper q-limit for $\alpha = 1$, indicates a cross-section size of the bundle, which was evaluated as $R_2 = 600\,\text{nm}$ ($= 2\pi/q_2$). As compared to the ribbon width, shown in Figure 3 determined by TEM for the dried cellulose ($= 100\,\text{nm}$), R_2 is much larger. $\alpha = 2.5$ in the lowest q-region is supposedly due to a gel network, composed of bundles. $\alpha = 2.35$ in the highest q-region is due to concentration fluctuations inside the swollen cellulose bundle and ribbon. The cellulose swollen by D_2O or pure D_2O has large scattering contrast against the crystallite. The power law of $\alpha = 2.35$ is limited by a hump appearing at q_1 ($= 0.07\,\text{Å}^{-1}$). The size R_1 ($= 2\pi/q_1$) is about 7 nm, which is equal to the crystallite width in the cellulose ribbon, as reported in reference [1].

For the dried cellulose, the power law q-behaviors were strongly affected, as indicated by filled circles in Figure 4. We found from higher q values, $\alpha = 4$ for $0.005 < q < 0.07\,\text{Å}^{-1}$, $\alpha = 2.4$ for $0.001 < q < 0.005\,\text{Å}^{-1}$, and $\alpha = 2.5$ for $0.00003 < q < 0.0008\,\text{Å}^{-1}$. We denoted the upper and lower limits for the power laws as q_5 and q_6 in Figure 4.

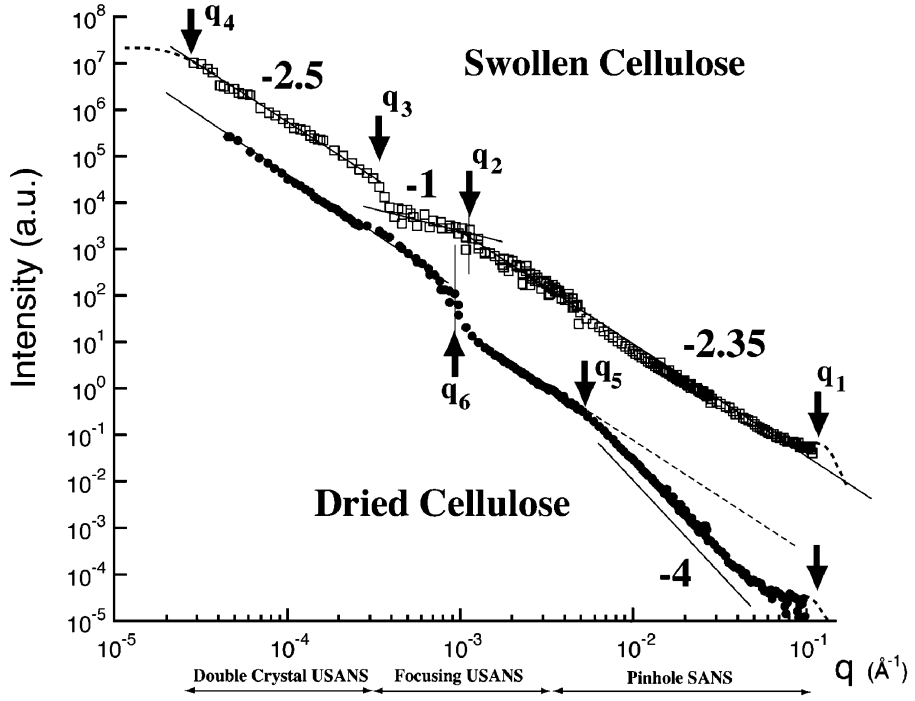

Fig. 4. Ultra-small–angle and small-angle neutron scattering, obtained for cellulose swollen by D_2O (open squares) and dried cellulose (filled circles).

In the highest q-region, we clearly observe Porod's law, showing an asymptotic decay of q^{-4}, originating from a sharp interface between dried cellulose. The space occupied by water might become vacant after drying. The upper q-limit for $\alpha = 4$ is close to q_1, and the hump at q_1 becomes more obvious as compared to the swollen cellulose. From the lower q-limit for $\alpha = 4$ (q_5), we evaluated $R_5 = 125\,\text{nm}$ ($= 2\pi/q_5$), which agrees well with the ribbon width observed in the TEM image in Figure 3. The network in the pellicle, the diameter of which was determined as $R = 600\,\text{nm}$, may be composed of several ribbons, the width of which was determined as $R = 125\,\text{nm}$ after drying. Thus the internal structure (or internal concentration fluctuations) of the cellulose bundle is strongly affected by drying. After drying, the q-region showing $\alpha = 2.5$ from the gel network increases from q_3 to q_t. This is due to the shrinkage of the gel network. This is why we cannot recognize α closer to 1 in the middle q-region, which we clearly observed for the swollen cellulose. If we compare two q values (q_3 and q_t), we obtain a swelling ratio $\gamma = 2.7$.

Figure 5 shows the power laws determined by USANS and SANS and schematically presents the hierarchical structures. For the swollen cellulose, $\alpha = 1$, found for $R_3 > R > R_2$, is attributed to the bundle composed of cellulose ribbons. $\alpha = 2.35$, found for $R_2 > R > R_1$, is attributed to the concentration fluctuations in the bundle, arising between crystallite and amorphous cellulose. From the upper limit q_1, we estimated $R_1 = 7\,\text{nm}$, which is close to the size of the crystallite (microfibril). Surprisingly, in the range $R_2 > R > R_1$, the size of the cellulose ribbon appears; however, the power law ($\alpha = 2.35$) does not change.

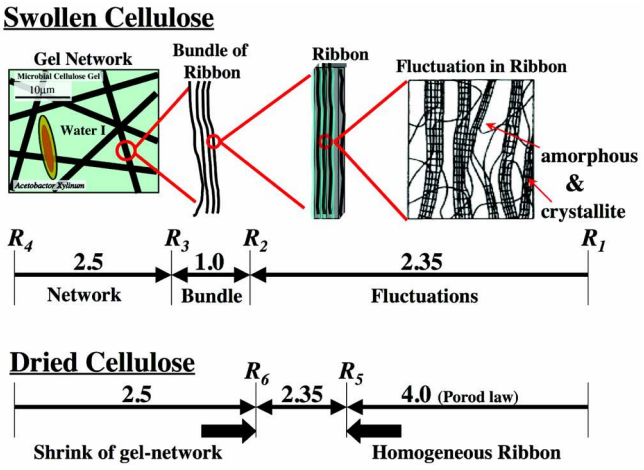

Fig. 5. Power law (α) and length scale limits, determined by USANS and SANS on swollen and dried cellulose.

For the dried cellulose, we found $\alpha = 4.0$ for $R < R_5$ at the highest q-region, which is Porod's law arising from a sharp interface. This is because for the dried specimen, crystallization is further developed and the space inside the ribbon becomes homogeneous. R_5 ($= 125\,\text{nm}$) is close to the width of the cellulose ribbons observed by TEM in Figure 3. However, for $R_6 > R > R_5$, the power law ($\alpha = 2.35$) does not change as compared to the swollen cellulose. This implies that the internal structure of the bundle, which is composed of ribbons, is not affected by drying. The amorphous domains occupied by water presumably remain. Instead of water, we find air (vacancy)

therein. The power law ($\alpha = 2.5$), originating from the network structure, appears at lower q and superimposes on the q-region where we found $\alpha = 1$ for the swollen specimen. This is due to shrinkage of the gel network by drying.

3.3 Fractal analysis

For the swollen and dried cellulose, we observed small-angle scattering, which obeys a power law q-behavior according to $\sim q^{-\alpha}$, with α varying between 1 and 3. We attribute the power laws between 1 and 3 to mass fractals [3] for spatial distribution of the center of mass for the crystallite in microbial cellulose. USANS and SANS arise from the scattering contrast between the crystalline and amorphous regions, both of which are, respectively, composed of pure cellulose and swollen cellulose or pure water.

According to the mass fractal, the total mass (or volume) $M(R)$ occupying a space of volume R^3 changes as R increases, as follows:

$$M(R) \sim R^{d_m}\,, \tag{1}$$

where d_m is the mass fractal dimension ($1 < d_m < 3$) and identical to the power law (α) determined by the small-angle scattering technique. It should be stressed that for a real system, we would find a mass fractal in between the upper and lower fractal length scale limits, $R_{\rm L}$ and $R_{\rm U}$, respectively. On the basis of the mass fractal, we evaluate a volume fraction of cellulose crystallite, $\phi(R)$, by simply normalizing $M(R)$ with R^3:

$$\phi(R) = \left(\frac{R}{R_{\rm L}}\right)^{-(3-d_m)} \qquad \text{for } R_{\rm L} < R < R_{\rm U}\,. \tag{2}$$

According to equation (2), $\phi(R)$ varies as we change the length scale of our observation R. Finally when R increases sufficiently, $\phi(R)$ reaches the bulk concentration $\phi_{\rm B}$ and is independent of R.

In Figure 6, we show $\phi(R)$ determined for the swollen and dried cellulose. For the swollen cellulose ((a) in Fig. 6), from at R_1 ($= 7\,$nm), $\phi(R)$ starts to decrease according to $R^{-0.65}$; the power of 0.65 was obtained from $3 - \alpha$ with $\alpha = 2.35$. At R_2 ($= 600\,$nm), the slope of $\phi(R)$ changes to 2 due to $\alpha = 1.0$ for the bundle structure. For $R_3 < R < R_4$, the slope of $\phi(R)$ is 0.5 due to $\alpha = 2.5$ for the network structure. Finally at $R_4 = 20\,\mu$m, $\phi(R)$ reaches 0.01, which is equivalent to $\phi_{\rm B}$ determined by weighing. For length scales larger than R_4, we expect that $\phi(R)$ is independent of R.

For the dried cellulose, $\phi(R)$ indicates the volume fraction of the cellulose ribbon. Therefore, $\phi(R)$ starts to decrease from the ribbon size R_6 ($= 125\,$nm) according to $R^{-0.65}$. For $R_6 < R < R_7$, $\phi(R)$ obeys $R^{-0.5}$. Finally at R_4 ($= 20\,\mu$m), $\phi(R)$ reaches 0.08, which is close to $\phi_{\rm B} = 0.055$, determined for the dried cellulose.

As shown in Figure 6, the microbial cellulose, synthesized and assembled by *A. xylinum*, shows a characteristic hierarchical structure of three different hierarchies:

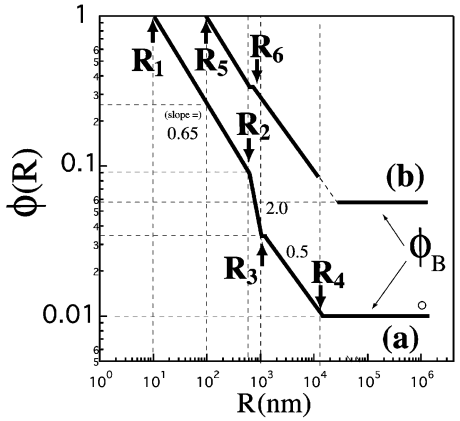

Fig. 6. Length scales-dependent concentration of the (a) crystallite and (b) ribbon, determined by USANS and SANS.

concentration fluctuations, bundle, and network. Surprisingly, we find that a large amount of water, about 90%, is involved in a bundle structure. The network structure, on the other hand, involves only 10% of the total water. In the intermediate hierarchy of the concentration fluctuations, we find the cellulose ribbon, which is recognized as a key unit of the microbial cellulose. The power law, due to the concentration fluctuations in a bundle ($\alpha = 2.35$), is not affected by the cellulose ribbon; for length scales larger or smaller than the ribbon size (R_5) we find $\alpha = 2.35$. However, if we remove water from the bundles for $R < R_5$, the concentration fluctuations disappear and the microbial cellulose becomes homogeneous, showing Porod scattering of $\alpha = 4.0$.

3.4 What determines the hierarchical structure of microbial cellulose? Interplay among physics, chemistry and biology

The hierarchical structure in microbial cellulose is determined by biogenic factors originating from *A. xylinum*, coupled with physicochemical factors. The sizes of the crystallite (R_1) might be affected by the pore size of the TC and its allocation on the outer membrane. The tablet shape of the cellulose ribbon might be related to the linear allocation of the TC. The concentration fluctuations in a cellulose bundle originate from the hierarchical order of amorphous regions, which is introduced during the course of crystallization or molecular assembly, forming a sub-elementary fibril and a microfibril.

In addition to the simultaneous and subsequent processes of polymerization, crystallization, and assembly, cell movement is also important for determining the hierarchy of microbial cellulose. The network structure, as determined in Figure 6, was obtained by static cultivation at the air surface of the culture medium, in which *A. xylinum* was able to move freely. In Figure 7, we illustrate a mechanism of bundle formation related to cell movement and cell division, which may simultaneously occur during

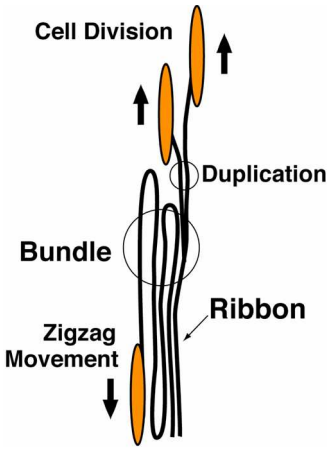

Fig. 7. Schematic diagram of a bundle formation process, related to cell movement and cell division.

cultivation. Due to the force of cellulose microfibril crystallization, *A. xylinum* moves along a previously formed cellulose ribbon. Zigzag movement along this previously formed cellulose ribbon makes the bundle of cellulose ribbons thicker. Cell division then duplicates the ribbon; the bridging ribbon seen in Figure 3 is presumably the result of cell division. For a length scale close to the ribbon size (R_5), the ribbons are coherently aligned. For length scales much larger than the ribbon size (R_5), the ribbons are incoherently allocated, giving rise to the network structure with $\alpha = 2.5$.

If we use a template to control cell movement, we are able to modify the network structure and its fractal dimension. For example, a honeycomb patterned cellulose network was fabricated by controlling the cell motion of *A. xylinum* on a patterned template [4]. The highly oriented cellulose is also obtained by employing a grooved substrate of polydimethylsiloxane (PDMS) [5]. Due to the excellent permeability of oxygen in PDMS, *A. xylinum* tends to attach to the PDMS surface because of its aerotactic nature and moves along the groove when we put the PDMS substrate at the interface between air and culture medium.

3.5 Comparison with enzymatic polymerization of cellulose

We now discuss the hierarchical structure of cellulose synthesized by a non-biosynthesis pathway (*in vitro* "enzymatic polymerization" of cellulose). Although the *in vitro* synthesis of cellulose has been the most challenging of research topics, the first successful achievement via an enzymatic reaction was reported in 1991 [6]. The reaction is designed to use the substrate of β-cellobiosyl fluoride, dissolved in the acetate buffer (CH_3COOH/CH_3COONa). To this solution, acetonitrile is added. The polymerization is initiated by mixing this substrate with an enzyme solution, unpurified cellulase obtained from *Trichoderma viride*.

In reference [7], we employed this enzymatic polymerization method to investigate the molecular assembly by small-angle scattering methods. The solution was transparent up to 2 h after starting the polymerization, but thereafter became opaque and turbid. As the polymerization further proceeded, white precipitates of the reaction product (polysaccharide) appeared in the solution, indicating that the self-assembly of cellulose synthesized by *in vitro* enzymatic polymerization is water-insoluble.

The precipitate was examined over a wide q-region by USANS and SANS, partially reinforced by small-angle or ultra-small–angle X-ray scattering (SAXS and USAXS) (see Fig. 10 in Ref. [7]). The scattering curve is described by a power law with $\alpha = 3.7$ for lower values of q, $\alpha = 2.1$ for middle q's, and finally $\alpha = 4$ at the highest q. $\alpha = 3.7$ and 4 found at the lowest and highest q's are attributed to the surface structure of the precipitate, according to the surface fractal, whose dimension is defined as $d_S = 6 - \alpha$. At the lowest q, the surface fractal dimension of the precipitate was determined as $d_s = 2.3$ $(= 6 - 3.7)$, implying a sharp surface of the crystallite. The appearance of a surface fractal, instead of the mass fractal dominantly observed for microbial cellulose, means that the precipitate is homogeneous and excludes water.

4 Conclusion

Using a ultra-small–angle neutron scattering technique, we examined the hierarchical amorphous domains in microbial cellulose over a wide range of length scales from nm to 10 μm. We determined three different hierarchical structures in the microbial cellulose, namely, a gel network, a single bundle composed of cellulose ribbons, and concentration fluctuations in a bundle. According to quantitative analyses on small-angle scattering based on a mass fractal and its length scale limits, it was determined that 90% of the cellulose bundle is occupied by amorphous cellulose.

References

1. C.H. Haigler, P.J. Weimer (Editors), *Biosynthesis and Biodegradation of Cellulose* (Marcel Dekker Inc., New York, 1991).
2. S. Koizumi, H. Iwase, J. Suzuki, T. Oku, R. Motokawa, H. Sasao, H. Tanaka, D. Yamaguchi, H.M. Shimizu, T. Hashimoto, J. Appl. Crystallogr. **40**, s474 (2007).
3. D. Avnir (Editor), *The Fractal Approach to Heterogeneous Chemistry* (John Wiley & Sons, 1989).
4. Wakako Kasai, Tetsuo Kondo, Macromol. Biosci. **4**, 17 (2004).
5. Putra Ananda *et al.*, submitted to *Biomacromolecules*.
6. S. Kobayashi, K. Kashiwa, T. Kawasaki, S. Shoda, J. Am. Chem. Soc. **113**, 3099 (1991).
7. Hirokazu Tanaka, Satoshi Koizumi, Takeji Hashimoto, Kazuhiro Kurosaki, Shiro Kobayashi, Macromolecules **40**, 6304 (2007).